Numerical study on rainfall infiltration in rock-soil slop

LIU Yuewu, LIU Qingquan, CHEN Huixin, GONG Xin, ZHANG Dawei, YAO Deliang & LI Lianxiang

Division of Engineering Science, Institute of Mechanics, Chinese Academy of Sciences, Beijing 100080, China

Correspondence should be addressed to Liu Yuewu (email: lywu@imech.ac.cn)

Received July 20, 2004; accepted November 9, 2004

Abstract A mathematical model for the rain infiltration in the rock-soil slop has been established and solved by using the finite element method. The unsteady water infiltrating process has been simulated to get water content both in the homogeneous and heterogeneous media. The simulated results show that the rock blocks in the rock-soil slop can cause the wetting front moving fast. If the rain intensity is increased, the saturated region will be formed quickly while other conditions are the same. If the rain intensity keeps a constant, it is possible to accelerate the generation of the saturated region by properly increasing the vertical filtration rate of the rock-soil slop. However, if the vertical filtration rate is so far greater than the rain intensity, it will be difficult to form the saturated region in the rock-soil slop. The numerical method was verified by comparing the calculation results with the field test data.

Keywords: rock-soil block, rainfall, water content, infiltration, Finite Element Method (FEM).

DOI: 10.1360/04zze18

1 Introduction

The effect of water on landslide stability has been paid much attention to for a long time. Water in landslide primarily comes from rainfall infiltration, ground water and other sources. Among them, the rainfall, which is a kind of uncontrollable external condition, is of significance for landslide failures. The landslide accidents induced by rainfall are possessed of a large proportion. Especially, the group landslides caused by rainfall commonly result in very serious hazard. However, since the effect of the rainfall infiltration on the slope stability is complex, it is necessary to study the mechanics of the rainfall infiltration.

The effect of rainfall on the stability of slopes is primarily reflected on the changes of pore pressure field, stress field, medium strength, and the dead weight of slope body caused by rainfall infiltration. Most of researches in the past focused on two aspects.

One is the macroscopic statistical analysis. It is mainly to determine the relationships between the landslide failure and the rainfall factors by analyzing a large amount of measured data[1~4]. The effect factors include the rainfall intensity, precipitation, frequency and so on. The other is the effect of pore pressure change caused by rainfall infiltration on the instability of landslides[5~9]. The investigation objects were mainly focused on both soil slopes and rock slopes. Relatively, it is scarce to investigate the meticulous process and mechanism of rainfall infiltration. Especially, there are fewer researches on the process of rainfall infiltration in the rock-soil slopes.

Rainfall infiltration is a typical unsaturated filtration process, which was extensively investigated by hydrologists and soil physicists in the last century. No matter in saturated or unsaturated zone, the water flow is obeyed the mass conservation law. The experiments demonstrated that Darcy's Law is appropriately tenable in unsaturated zone. Richards[10] first introduced the Darcy's Law to the unsaturated filtration in soil and derived the well-known Richards Equation. Horton[11] did more deliberate researches on the infiltration process in surface soil and obtained the law of the infiltration rate. He pointed out that there exists a maximum infiltration rate curve for any given soils. For heavy rain, the practical process of infiltration is in compliance with this maximum infiltration rate curve, which was called the "infiltration capacity curve of soil". During the process of infiltration, the infiltration capacity reduces gradually and finally reaches a constant value. This process depends on the initial porosity, water content and the feature of soil. Many laboratory tests demonstrated that the infiltration rate decreases faster for the clay soil with minute pores than that of the sandy soil with coarse pores, but the final constant value of the former is lower. When the rainfall intensity exceeds the infiltration capacity of soil, the redundant rainwater becomes the overland flow on the surface. The investigation by Rubin and other scholars[12~14] made the great progress on soil infiltration. Their research indicated that when rainfall intensity, the initial water condition in soil and the unsaturated characteristic curve of soil are given, Horton's[11] maximum infiltration rate curve can be predicted theoretically and the final constant infiltration rate will be equal to the unsaturated hydraulic conductivity.

The infiltration capacity of soil is an empirical concept in hydrology, but it has strict definition in soil physics with the movement process of the unsaturated ground water. Most of the researches focused on one-dimensional vertical infiltration in the past. Bodman and Colman[15] conducted the empirical analysis for the first time. Subsequently, Philip[16~23] applied the analytic method to resolve the one-dimensional boundary value problem, and discovered the basic mechanism of this issue, which settled the foundation for theoretical analysis. Freeze[24~26] reviewed the early investigations on soil infiltration and concluded that the one-dimensional infiltration problem in the saturated-unsaturated system is controlled by the equation $\partial/\partial z[k(\varphi)(\partial\varphi/\partial z+1)]=C(\varphi)\partial\varphi/\partial t$, where $\varphi=h-z$ is the pressure head; $k(\varphi)$ and $C(\varphi)$ are the unsaturated functions of hydraulic conductivity and water content, respectively. In the saturated zone below the

level of ground water (or $\varphi = \varphi_a$, where φ_a is the pressure head for the air enters the soil), $k(\varphi)$ is a constant k_0 and $C(\varphi) = 0$ (k_0 is the hydraulic conductivity of the saturated zone). However, they claimed that the analytic method is unsuitable to deal with the two-dimensional or three-dimensional issue. So the numerical simulation becomes an important method to study the complicated process of soil infiltration.

The investigations on 1-D infiltration in homogeneous isotropic soil have been developed perfectly in the last century. But the researches on homogeneous anisotropic soil and heterogeneous media are rather limited. The research on the water flow in homogeneous anisotropic soil began in the 1950s, and the research methods are primarily the coordinate conversion methods. Among them, the achievements made by Maasland, Bear, Dagan and Liakopoulos are the most representative. Bear[27] made a relative comprehensive discussion. However, till now, the research on the anisotropic system is still rare, especially for the rock-soil media containing a large amount of rock blocks. The key problem of this issue is the mechanism of the unsteady infiltration in complex porous media. The description of the homogeneous porous media, such as soil or rock, is relatively easy and successfully developed. However, the description of the heterogeneous porous media such as the rock-soil slop is relatively difficult, so that there is no relatively suitable theoretical achievement. Most slopes in the Three Gorges Reservoir region are ancient landslide congeries consist of rock-soil masses. To discuss the mechanism of rainfall effecting on the landslide stability, it is necessary to carefully study the infiltration mechanism in the special heterogeneous media. In recent years, much attention was paid on this issue. Zhang et al.[28], for example, made some field test on the rainfall infiltration in these kinds of slopes and collected a large number of test data. However, in general, since the rainfall infiltration process in the rock-soil slopes is extremely complex, most of the present results cannot be applied to this issue and more comprehensive analysis and research are needed.

Based on this background of rock-soil slopes in the Three Gorges Reservoir region, a mathematical model for rainfall infiltration in the rock-soil slopes is established by simplifying the rock blocks as impervious mass in this paper. The finite element numerical method was used to solve the problem. The mechanism of rainfall infiltration in the rock-soil slop was analyzed in detail by considering the changes of infiltration strength and vertical infiltration rate of soil. The researches results are the fundamental base for analyzing the effect of rainfall on the slope stability and the mechanism of landslide failures caused by rainfall.

2 Mathematical model

2.1 Governing equations

One of the key problems for investigating rainfall infiltration in the rock-soil slop is how to reasonably describe the heterogeneity of porous media. The existence of a large amount of rock blocks in soil makes the infiltration rate used in the homogeneous media

useless. The method of equivalent media is one of the adopted methods for the heterogeneous media in the past. That is to say, the infiltration theory obtained in the homogeneous media is still used in the heterogeneous media by considering the concept of an equivalent average infiltration rate. But the equivalent average infiltration rate is affected greatly by the characteristic of media such as the greatly varied of rock blocks. Therefore, it is unsuitable for processing the infiltration problem in the heterogeneous media, especially for the rock-soil slop. To study the infiltration feature in this kind of heterogeneous media, we consider the rock blocks as the impervious blocks. Further more, their shape is simplified to a square, while the soil is still treated as homogeneous media. This approximate method is useful to resolve the infiltration process in the rock-soil media. The research region is selected as a rectangular section with some section with some rock blocks randomly distributed in the whole area (Fig. 1).

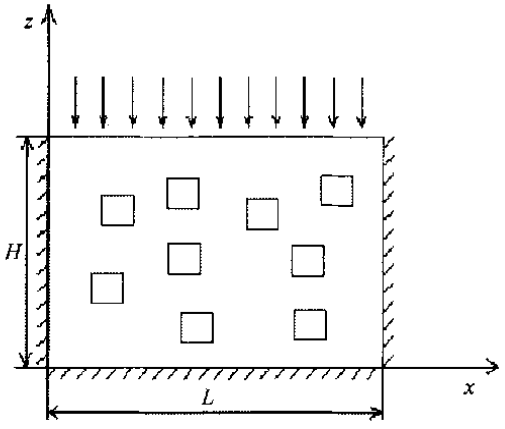

Fig. 1. Schematic of physical model.

Based on Richards's theory[10], at the beginning of rainfall stage, the infiltration capacity on the surface of the rock-soil slop is relatively large and the vertical infiltration rate is equal to the rainfall intensity. Then, the boundary condition on the surface can be described as the second type boundary condition. With the evolution of the infiltration, the pores in soil are gradually filled up by water. The water content, pressure head and hydraulic head increase as well, but the downward hydraulic gradient reduces and the infiltration capacity on surface of the rock-soil slop reduces subsequently. When the surface infiltration rate is less than rainfall intensity, rainwater will accumulate on the surface resulting in surface runoff. At this time, the water content in the surface of the rock-soil slop reaches saturation, and the boundary condition of ground surface can be described with second type boundary condition. Therefore, the basic mathematic model of this issue can be described as the following Richards equation[10]:

$$\frac{\partial}{\partial x}\left(D_x(\theta)\frac{\partial \theta}{\partial x}\right)+\frac{\partial}{\partial z}\left(D_z(\theta)\frac{\partial \theta}{\partial z}\right)-\frac{\partial k_z(\theta)}{\partial z}=\frac{\partial \theta}{\partial t}, \tag{1}$$

where θ is the water content; θ_s is the saturated water content, $D_x(\theta)$ and $D_z(\theta)$ are the diffusion coefficients of unsaturated soil in the horizontal and vertical directions, respectively, and $k_z(\theta)$is the permeability coefficient of unsaturated soil.

For this study, the right, left and bottom edges of the calculation field are imperious, and the initial water content is 0. The following boundary and initial conditions can be derived:

$$\frac{\partial \theta}{\partial x}=0, \quad x=0, x=L, \tag{2}$$

$$D_z(\theta)\frac{\partial \theta}{\partial z}-k_z(\theta)=-R(t), \quad z=H, \quad 0<t<t_a, \tag{3}$$

$$\theta=\theta_s, \quad z=H, \quad t>t_a, \tag{4}$$

$$\frac{\partial \theta}{\partial z}=0, \quad z=0, \tag{5}$$

$$\theta_I = 0, \ t = 0, \tag{6}$$

where L is the model length, H is the model thickness, R is the rainfall intensity, t_a is the time that the surface layer reaches saturation.

2.2 Finite element method

Finite element method (FEM) is used to solve the above infiltration equations. FEM was first introduced by Javandel and Witherspoon[29] into their research and was widely used to study ground water. Based on the Galerkin method, the linear interpolating function φ_i is selected as the weighting function. Let the integral in the weighting margin in the unit region equal 0, that is

$$\iint_A \varphi_i^e\left(\frac{\partial}{\partial x}\left(D_x(\theta)\frac{\partial \theta}{\partial x}\right)+\frac{\partial}{\partial z}\left(D_z(\theta)\frac{\partial \theta}{\partial z}\right)-\frac{\partial k_z(\theta)}{\partial z}-\frac{\partial \theta}{\partial t}\right)\mathrm{d}x\mathrm{d}z=0, \ \ i = 1, 2, 3, \tag{7}$$

where φ_i^e is the unit linear interpolating function: $\varphi_i^e = a_i + b_i x + c_i z$, $(i = 1, 2, 3)$.

$$\frac{\partial \varphi_i^e}{\partial x}=b_i, \quad \frac{\partial \varphi_i^e}{\partial z}=c_i, \quad a_i=\frac{1}{2A}(x_j z_k - x_k z_j), \quad b_i=\frac{1}{2A}(z_j - z_k), \quad c_i=\frac{1}{2A}(x_k - x_j), \tag{8}$$

where A is the area of the triangle element:

$$A=\frac{1}{2}\begin{vmatrix}1 & 1 & 1\\ x_i & x_j & x_k\\ z_i & z_j & z_k\end{vmatrix}. \tag{9}$$

Let $\theta^e=\theta_i^e\varphi_i^e+\theta_j^e\varphi_j^e+\theta_k^e\varphi_k^e$ (where θ_i^e, θ_j^e, θ_k^e are the water content at the three nodes of the element, respectively), then

$$\frac{\partial \theta^e}{\partial x}=\theta_i^e\frac{\partial \varphi_i^e}{\partial x}+\theta_j^e\frac{\partial \varphi_j^e}{\partial x}+\theta_k^e\frac{\partial \varphi_k^e}{\partial x}, \tag{10}$$

$$\frac{\partial \theta^e}{\partial z} = \theta_i^e \frac{\partial \varphi_i^e}{\partial z} + \theta_j^e \frac{\partial \varphi_j^e}{\partial z} + \theta_k^e \frac{\partial \varphi_k^e}{\partial z}. \tag{11}$$

Using Green's formula and assuming the change rates of D_x, D_z and k_z in the triangular finite element as constants respectively, the finite element equation of the issue can be obtained as:

$$\iint_A \varphi_i^e \left[\frac{\partial D_x}{\partial x} \cdot \frac{\partial \theta}{\partial x} + \frac{\partial D_z}{\partial z} \cdot \frac{\partial \theta}{\partial z} \right] \mathrm{d}x\mathrm{d}z - \iint_A \left[D_x(\theta) \frac{\partial \varphi_i^e}{\partial x} \cdot \frac{\partial \theta^e}{\partial x} + D_z(\theta) \frac{\partial \varphi_i^e}{\partial z} \cdot \frac{\partial \theta^e}{\partial z} \right] \mathrm{d}x\mathrm{d}z -$$

$$\left[k_z(\theta) - R(t) \right] \cdot \frac{L}{2} - \frac{\partial k_z}{\partial z} \iint_A \varphi_i^e \mathrm{d}x\mathrm{d}z -$$

$$\left[\frac{\partial \theta_1^e}{\partial t} \iint_A \varphi_i^e \varphi_1^e \mathrm{d}x\mathrm{d}z + \frac{\partial \theta_2^e}{\partial t} \iint_A \varphi_i^e \varphi_2^e \mathrm{d}x\mathrm{d}z + \frac{\partial \theta_3^e}{\partial t} \iint_A \varphi_i^e \varphi_3^e \mathrm{d}x\mathrm{d}z \right] = 0, \tag{12}$$

where $\int_\Gamma \varphi_i^e \mathrm{d}s = \frac{L}{2}$, L is the distance between every two nodes in the triangle element.

$$\iint_A \varphi_i^e \varphi_j^e dA = \begin{cases} \frac{A}{6} (i = j), \frac{\partial \theta_i^e}{\partial t} = \frac{\theta_i^{e,n+1} - \theta_i^{e,n}}{\Delta t}, \\ \frac{A}{12} (i \neq j). \end{cases} \tag{13}$$

Let $PDX = \partial D_x / \partial x$, $PDZ = \partial D_Z / \partial Z$, $KZZ = \partial k_z / \partial z$, $KDZ = k_z(\theta) / D_z(\theta)$, $NDZ = 1 / D_z(\theta)$, the eq. (7) can be rewrite as:

$$\left[PDX \cdot (\theta_1 b_1 + \theta_2 b_2 + \theta_3 b_3) + PDZ (\theta_1 c_1 + \theta_2 c_2 + \theta_3 c_3) \right] \cdot \frac{1}{3} A -$$

$$\left[D_x(\theta) \cdot b_i \cdot (\theta_1 b_1 + \theta_2 b_2 + \theta_3 b_3) + D_Z(\theta) \cdot c_i \cdot (\theta_1 c_1 + \theta_2 c_2 + \theta_3 c_3) \right] \cdot A + \left[k_z(\theta) - R(t) \right] \cdot \frac{L}{2} -$$

$$KZZ \iint_A \varphi_i^e \mathrm{d}x\mathrm{d}z - \left[\frac{\partial \theta_1^e}{\partial t} \iint_A \varphi_i^e \varphi_1^e \mathrm{d}x\mathrm{d}z + \frac{\partial \theta_2^e}{\partial t} \iint_A \varphi_i^e \varphi_2^e \mathrm{d}x\mathrm{d}z + \frac{\partial \theta_3^e}{\partial t} \iint_A \varphi_i^e \varphi_3^e \mathrm{d}x\mathrm{d}z \right] = 0. \tag{14}$$

3 Simulation and analysis

For comparison, the rainfall infiltration processes in both the homogeneous and heterogeneous media were simulated numerically. The non-structure triangular meshes for both of them were generated by using the automatic generation method[30,31]. They are shown in Fig. 2.

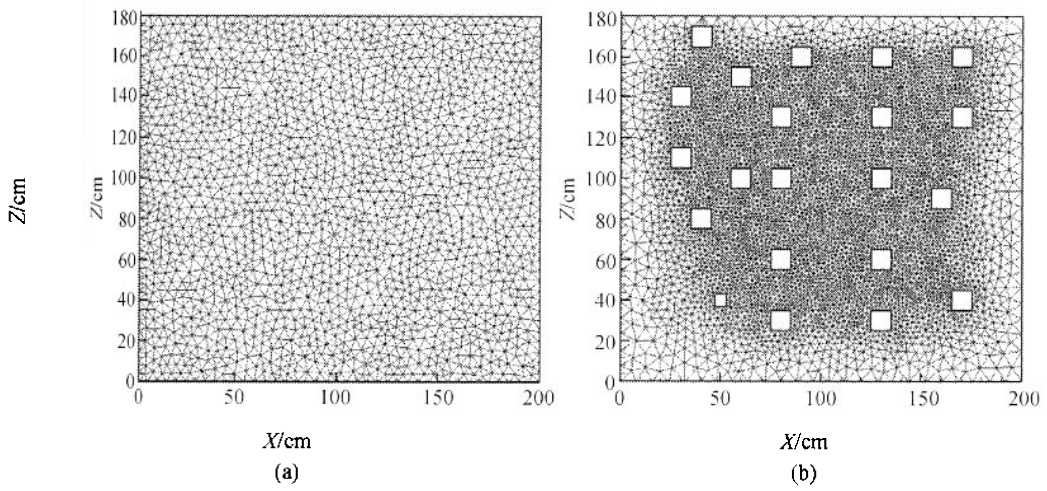

Fig. 2. Triangular non-structured meshes for the finite element method. (a) Meshes for homogenous soil; (b) meshes for rock-soil.

3.1 Rainfall infiltration in homogeneous media

The rainfall infiltration in the homogeneous soil was numerically simulated firstly. The fundamental parameters selected in the calculation are: $a=c=10.25$; $b=d=3.6$; $e=0.0379$; $f=3.487$; $R(t)=10^{-6}$ ms^{-1}; $H=180$ cm and $L=200$ cm. The simulation results of water content distributions are shown in Fig. 3. Fig. 3(a)—(d) are the distributions of water content at different times during the rainfall process. It can be seen that the process of rainfall infiltration evaluated slowly from the top to the bottom. During the process of rainfall infiltration, the water content near the surface layer increases gradually. Additionally, the contours of water content are nearly parallel to the surface. The greater the infiltration rate is, the more apparent the trend is. If the length in x direction is infinite, the contours of water content will be completely parallel to the surface of the model. When the porous media is saturated, the water content at the saturated point will no longer increase. Since the right and left edges of the calculation model are closed, their water contents increase slowly than those of other point.

3.2 Rainfall infiltration in heterogeneous media

Selecting the same fundamental parameters and taking each rock block as an impervious square, the process of rainfall infiltration in the rock-soil slop was also simulated. The simulation results of water content distributions are shown in Fig. 4. Fig. 4(a)—(d) are the water content distributions at different times during rainfall process. Similar to the process of rainfall infiltration in the homogeneous media, the infiltration process in the rock-soil is also a slow evaluating process from the top to the bottom. The water content near the surface layer increases gradually and the contours of water content are nearly parallel to the surface of the formation. In the early stage of rainfall infiltration process, i.e. before the wetting front of infiltration rainwater reach the impervious squares, the contours of water content share the similar trend with that of the homoge-

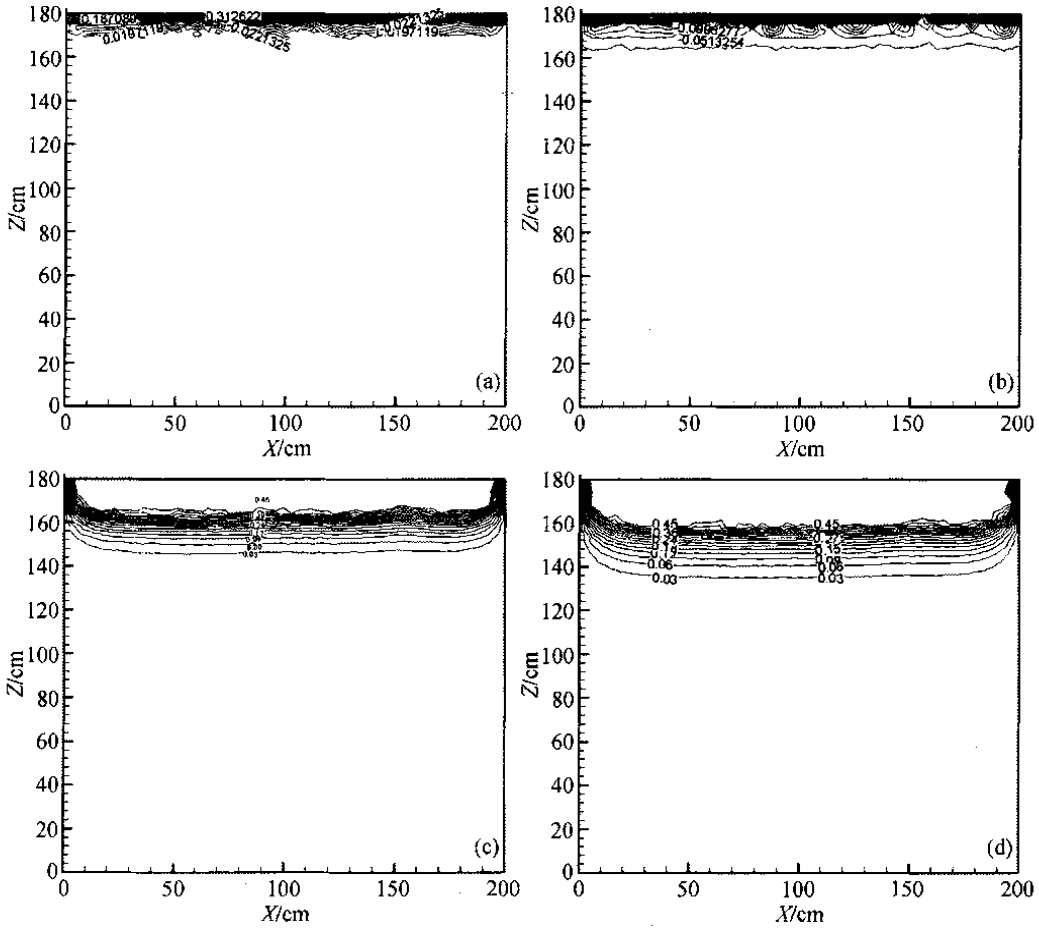

Fig. 3. Simulation results of infiltration process in the homogeneous soil. (a) Water content distribution at $t1$=1 h; (b) water content distribution at $t2$=10 h; (c) water content distribution at $t3$=63.1 h; (d) water content distribution at $t4$=100 h.

neous media (Fig. 4(a)). With the increase of rainfall precipitation, the wetting front of rainwater gradually reached to the impervious squares. At this time, the contours of water content appeared the trend of inclining to the impervious squares, which likes that the impervious blocks have the absorbing power (Fig. 4(b)). When the wetting front of rainwater exceeds the entire impervious blocks, the contours of water content appear as "warping", which likes that the impervious blocks impede the evolution of rainwater wetting front. In fact, the calculation results of water content contours show that the wetting front of rainfall infiltration develops more rapidly (Fig. 4(c)). When the water content reached saturation, the water content at the saturated point no longer increases (Fig. 4(d)). Similarly, because the right and left edges of the calculation model are closed, the water contents at these points are increased slowly.

3.3 Comparison and discussion

The simulated results of the water content distribution with X=100 cm at different times are shown in Fig. 5. The symbols ◇, ○, □ and △in Fig. 5 represent the simu-

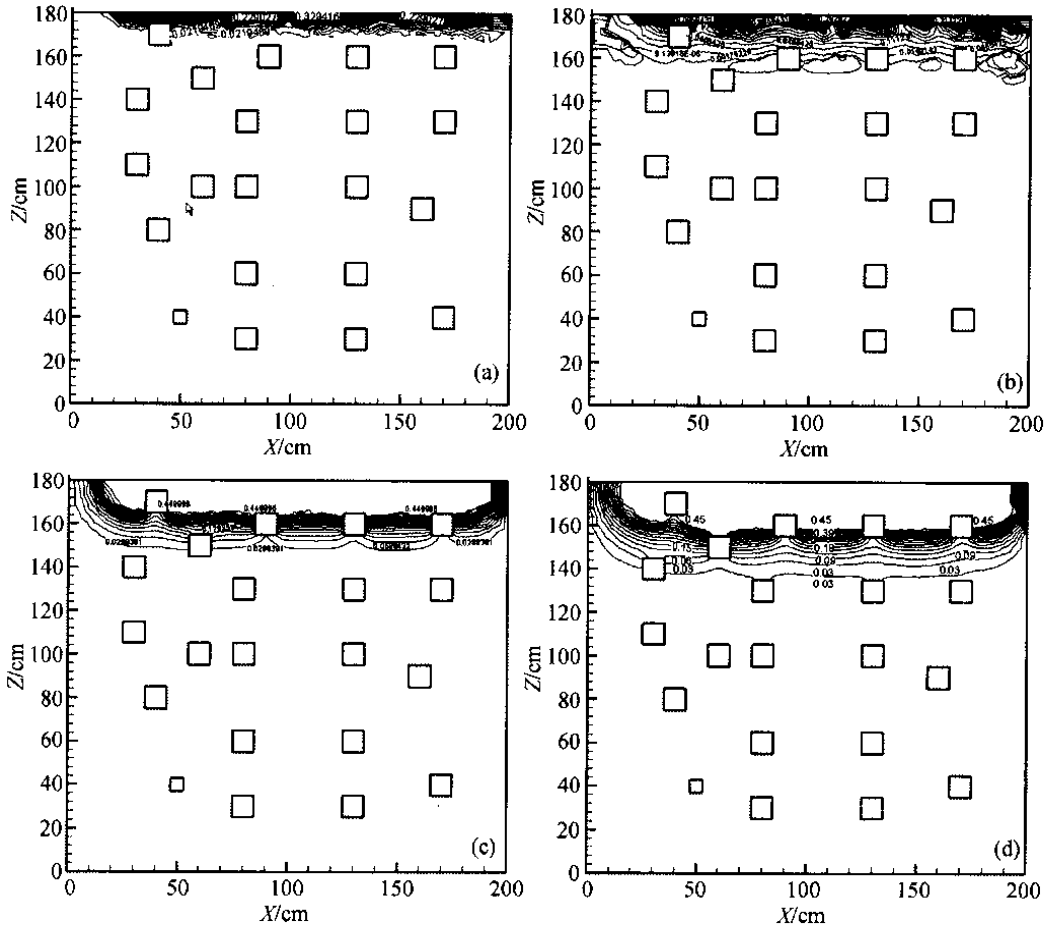

Fig. 4. Simulation results of rainfall infiltration process in the rock-soil slop. (a) Water content distribution at $t1$= 1 h; (b) water content distribution at $t2$=10 h; (c) water content distribution at $t3$=63.1 h; (d) water content distribution at $t4$=100 h.

lation results in the homogeneous media at times $t1$=1 h, $t2$=10 h, $t3$=63.1 h and $t4$=100 h, respectively, while ◆, ●, ■ and ▲represent the simulation results in the heterogeneous media at times $t1$=1 h, $t2$=10 h, $t3$=63.1 h and $t4$=100 h, respectively.

The simulated results show that: (i) In the early stage of rainfall infiltration, the variation of water content curves in the whole calculated region is not obvious. From $t1$=1 h to $t2$=10 h, the water content profile in the homogeneous media and the heterogeneous media are nearly the same. Actually, before $t2$=10 h, the wetting front of infiltration does not yet reach the impervious blocks, the infiltration velocities of both models are nearly perfectly agreeable. (ii) The water content at the same depth increases with time, because the rainfall infiltration process is an unsteady one. (iii) When $t2>10$ h, $\theta_{\text{rock-soil}}>\theta_{\text{soil}}$, the averaged infiltration coefficient of heterogeneous media is greater than that of the homogeneous media. Additionally, the depth of wetted front in the heterogeneous media is greater than that in the homogeneous media at the same period. (iv) In the later stage of rainfall infiltration, the water content at a certain distance from the ground surface

gradually reaches saturation, the water content curve becomes a strait line, i.e. the water content does not change with depth. The saturated region in the heterogeneous media is larger than that in the homogeneous media at the same time. This indicates that the averaged infiltration velocity in the heterogeneous media is greater than that in the homogeneous media. This conclusion is of signification to understand the mechanism of infiltration in the rock-soil slop.

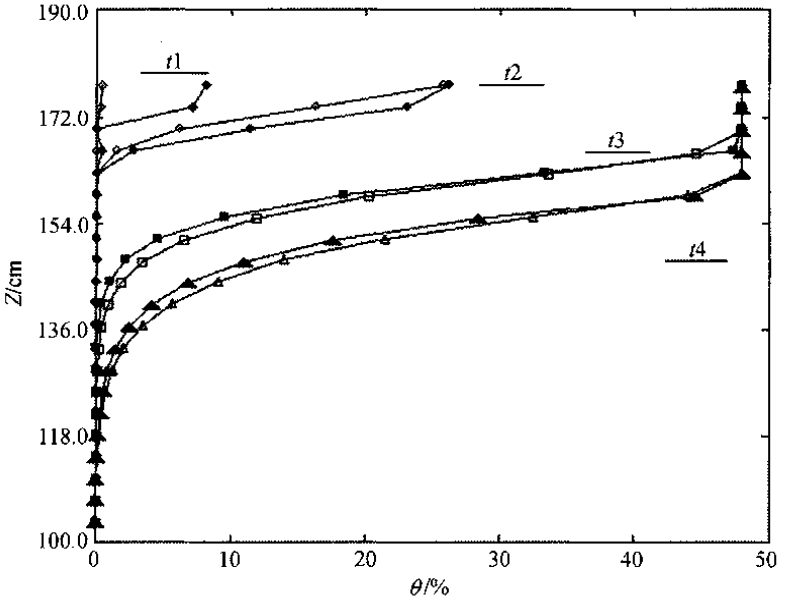

Fig. 5. Comparison of infiltration profiles between in the homogeneous soil and in the rock-soil slop.

3.4 Factor analysis

Different rainfall intensities and vertical infiltration rates are selected to simulate rainfall infiltration process in the heterogeneous rock-soil slop. The profiles of water content at $X=100$ cm as $t3=63.1$ h are shown in Fig. 6. In Fig 6, ○and ● represent the rainfall intensities $R=10^{-6}$ ms^{-1} and $R=10^{-5}$ ms^{-1} respectively. Fig. 7 shows the profiles of water content for different vertical infiltration rates, where ○and ● represent the infiltration rates $k=10^{-6}$ ms^{-1} and $k=10^{-5}$ ms^{-1} respectively.

It shows clearly that if other conditions are the same, the greater the rainfall intensity, the larger the saturated region. Similarly, the greater the infiltration rate, the deeper the wetted front.

3.5 Special simulation case

A special case in which the infiltration rate in the heterogeneous rock-soil slop is much larger than the rainfall intensity has been simulated. In this case, no water accumulation and surface runoff will be formed on the surface. The process of infiltration at the extreme condition was simulated and analyzed. In the simulation, the only changed condition is that the vertical infiltration rate k_z changed from 10^{-6} ms^{-1} to 10^{-3} ms^{-1}. Fig.

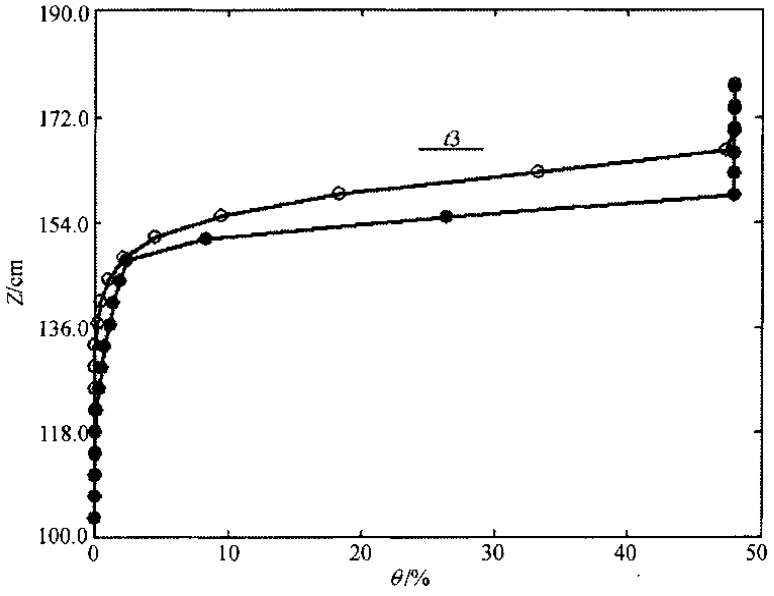

Fig. 6. Vertical distributions of water content for different rainfall intensities at t=63.1 h

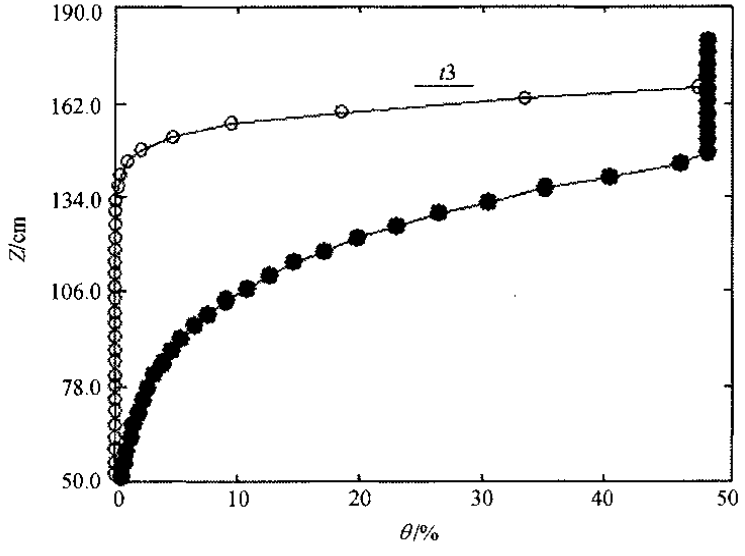

Fig. 7. Profile of water content for different infiltration rates at t=63.1 h.

8(a) is the simulated water content distribution in the rock-soil slop. Selecting X = 100 cm, the profile of water content at $t3$ = 63.1 h was plotted in Fig. 8(b). Curve 1 represents the profile of water content with $k_z = 10^{-3}$ ms^{-1} and $R = 10^{-6}$ ms^{-1}; curve 2 is the profile of water content with $k_z = 10^{-5}$ ms^{-1}and R=10^{-6} ms^{-1}; curve 3 is the profile of water content with $k_z = 10^{-6}$ ms^{-1}, $R = 10^{-6}$ ms^{-1}.

From Fig. 8(a), it can be seen that there is no saturated zone formed near the ground surface even till $t4$=63.1 h, just like the infiltration in the desert. Fig. 8(b) shows that the water content does not exceed 20% all the time (curve 1) under this condition, but re-

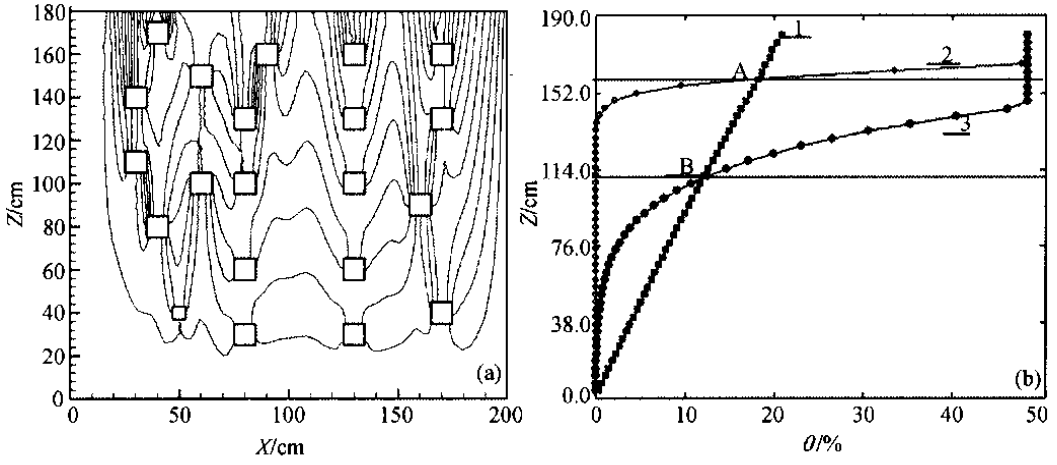

Fig. 8. Simulation results when vertical infiltration rate is more than rainfall intensity. (a) Water content distribution at t=63.1 h; (b) profiles of water content at t=63.1 h.

mains a relatively low value. It suggests that if the vertical infiltration rate is far greater than the rainfall intensity, the vertical infiltration rate dominates the whole process of infiltration. There are two points of intersection in Fig. 8(b), which are A(0.175, 159.0) and B(0.120, 110.3). Points A and B show that if the vertical infiltration rate is far greater than the rainfall intensity, the water content is smaller than that of the lower vertical infiltration rate case at the same depth within the range of distance from the surface to the point of intersection. The water content is greater than that of the lower vertical infiltration rate case at the same depth beyond the range of distance from the surface to the point of intersection. Curve 1 shows that the rainwater infiltrates rapidly and cannot form a saturated zone in the rock-soil slop. Curves 2 and 3 show that if the rainfall intensity remains constant, it is favorable to quickly form a saturated zone for the rock-soil slop to moderately increase the vertical infiltration rate.

3.6 Comparison with the field test data

The field test data of rainfall infiltration given by Zhang et al.[28] in a rock-soil slope in Three Gorges Reservoir region was selected to verify the numerical model established in this paper. Basing on the test results of Zhang et al.[28], the infiltration process in the rock-soil slop was simulated by selecting the infiltration rate of 1.465×10^{-6} ms^{-1}, the rainfall intensity of 1.465×10^{-6} ms^{-1} and the initial water content of zero. Fig. 9(a) shows the simulation results of the profile of water content at different times at X=100 cm, and Fig. 9(b) is the measured results in ref. [28]. By comparing these two results, it can be seen that the shapes and the values of two groups of curves are extremely similar and the changing process of water content is also agreeable. The difference of absolute values primarily comes from the initial water content (which was selected as zero in the calculation). Nevertheless, the comparison demonstrated that the model established in the paper is suitable to be used to simulate the rainfall infiltration process in the heterogeneous rock-soil slop.

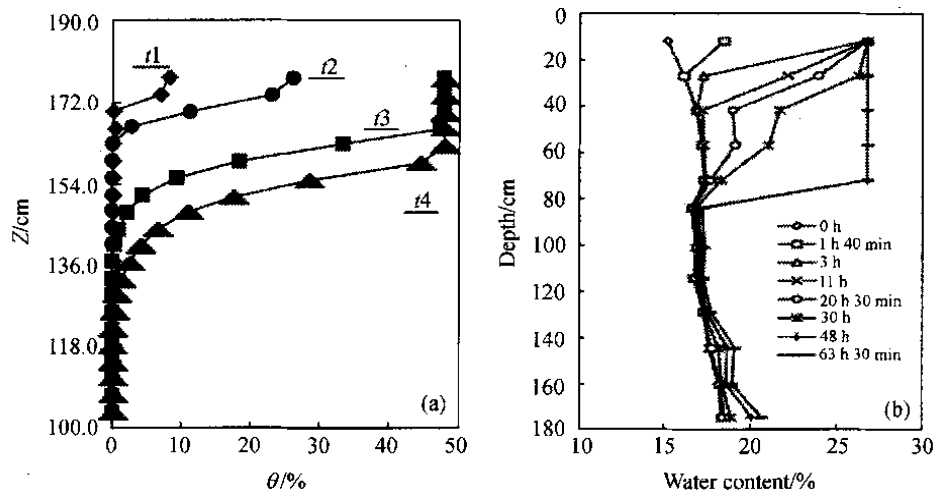

Fig. 9. Comparison of theoretical field test profile of water content. (a) Simulated results in this paper; (b) field test data in ref. [28].

4 Conclusions

(i) A mathematical model for simulating the process of rainfall infiltration in the rock-soil slop has been established and solved by FEM.

(ii) The simulated results show that the changing of water content in the rock-soil slop is unsteady and the existence of impervious blocks accelerates the velocity of rainfall infiltration.

(iii) If the other conditions are the same, it is easy to form saturated zone in the rock-soil slop by increasing rainfall intensity in the simulated model. The greater the rainfall infiltration is, the easier the saturated region forms in the rock-soil slop.

(iv) If the vertical infiltration rate is far greater than the rainfall intensity, the infiltration rate in the rock-soil slop primarily depends on the rainfall intensity. The infiltration velocity is accelerated apparently, but it is hard to form a saturated zone in the rock-soil slop.

(v) By comparing the simulation results with the field test data, we suggest that the simulation model established in the paper can be used to simulate the rainfall infiltration process in the heterogeneous media.

Acknowledgements The authors wish to thank all their colleagues in the Institute of Mechanics, CAS, for their valuable discussion on various parts of the work described in the paper. This work was supported by the Special Funds for Major State Basic Research Project (Grant No. 2002CB412703), the Knowledge Innovation Project of Chinese Academy of Sciences (Grant No. KJCX2-SW-L1-4) and the National Natural Science Foundation of China (Grant No. 10372104).

References

1. Iverson, R. M., Landslide triggering by rain infiltration, Water Resources Research, 2000, 36(7): 1897—1910.
2. Dykes, A. P., Weathering-limited rainfall-triggered shallow mass movements in undisturbed steepland tropical

rainforest, Geomorphology, 2002, 46: 73—93.
3. Iida, T., Stochastic, A., Hydro-geomorphological model for shallow landslide due to rainstorm, Catena, 1999, 34: 293—313.
4. Chen, H., Lee, C. F., A dynamic model for rainfall-induced landslides on natural slopes, Geomorphology, 2003, 51: 269—288.
5. Hanenberg, W. C., Observation and analysis of pore pressure fluctuations in a thin colluvium landslide complex near Cincinnati Ohio, Engineering Geology, 1991, 31: 159—84.
6. Iverson, R. M., Landslide triggering by rain infiltration, Water Resources Research, 2000, 36 (7): 1897—1910.
7. Montgomery, D. R., Dietrich, W. E., A physically based model for the topographic control on shallow landsliding, Water Resources Research, 1994, 30 (4): 1153—1171.
8. Torres, R., Dietrich, W. E., Montgomery, D. R. et al., Unsaturated zone processes and the hydrologic response of a steep unchanneled cathment, Water Resources Research, 1998, 34 (8): 1865—1879.
9. Angeli, M. G., Pasuto, A., Silvano, S., A critical review of landslide monitoring experiences, Engineering Geology, 2000, 55: 133—147.
10. Richards, L. A., Capillary conduction of liquid through porous mediums, Physics, 1931, 1: 318—333.
11. Horton, R. E., An approach towards a physical interpretation of infiltration-capacity, Soil. Sci. Soc. Am. Proc., 1940, 5: 399—417.
12. Rubin, J., Steinhardt, R., Soil water relation during rain infiltration, I. Theory, Soil Sci. Soc. Amer. Proc., 1963, 27: 246—251.
13. Rubin, J., Steinhardt, R., Soil water relation during rain infiltration, II. Moisture content profiles during rains of low intensities, Soil. Sci. Soc. Amer. Proc., 1964, 28: 1—5.
14. Rubin, J., Theoretical analysis of two-dimensional transient flow of water in unsaturated and partly unsaturated soils, Soil. Sci. Soc. Amer. Proc., 1968, 32: 607—615.
15. Bodman, G. B., Colman, E. A., Moisture and energy conditions during downward entry of water into soils, Soil. Sci. Soc. Amer. Proc., 1943, 8: 116—122.
16. Philip, J. R., The theory of infiltration: 1. The infiltration equation and its solution, Soil. Sci., 1957, 83: 345—357.
17. Philip, J. R., The theory of infiltration: 2. The profile at infinity, Soil Sci., 1957, 83: 435—448.
18. Philip, J. R., The theory of infiltration: 3. Moisture profiles and relation to experiment, Soil Sci., 1957, 84: 163—178.
19. Philip, J. R., The theory of infiltration: 4. Sorptivity and algebraic infiltration equations, Soil Sci., 1957, 84: 257—264.
20. Philip, J. R., The theory of infiltration: 5. The influence of initial moisture content, Soil Sci., 1957, 84: 329—339.
21. Philip, J. R., The theory of infiltration: 6. Effect of water depth over soil, Soil Sci., 1958, 85: 278—286.
22. Philip, J. R., Evaporation and moisture and heat field in the soil, J. Meteor., 1957, 14: 354—366.
23. Philip, J. R., de Vries, D. A., Moisture movement in porous materials under temperature gradients, Trans. Amer. Geophys. Union, 1958, 38: 222—232.
24. Freeze, R. A., The mechanism of nature groundwater recharge and discharge: 1. One-dimensional, vertical, unsteady, unsaturated flow above a recharging or discharging groundwater flow system, Water Res., 1969, 5: 153—17.
25. Freeze, R. A., Three-dimensional transient saturated-unsaturated flow in a ground basin, Water Resources Res., 1971, 7: 347—366.
26. Freeze, R. A., Influence of the unsaturated flow domain on seepage through earth dams, Water Resources Res., 1971, 7: 929—941.
27. Bear, J., Dynamic of Fluid in Porous Media, New York: Elsevier, 1972.
28. Zhang, J., Jiao, J. J., Yang, J., *In situ* rainfall infiltration studies at a hillside in Hubei Province, China, Engineering Geology, 2000, 57(1-2): 31—38.
29. Javandel, I., Witherspoon, P. A., A method of analyzing transient fluid in multilayered aquifers, Water Resources Res., 1969, 5: 856—869.
30. Zhu, J. Z., A new approach to the development of automatic quadrilateral mesh generation, International Journal for Numerical Methods in Engineering, 1991, 32: 849—866.
31. Wilson, E. L., Automation of the finite element method —— A personal historical view, Finite Elements in Analysis and Design, 1993, 13: 91—104.